1 # Mutations in the Histone Methyltransferase Gene, *KMT2B* Cause

2 # Early Onset Dystonia

3

4 [1]Meyer E[^], [2,3]Carss KJ[^], [4]Rankin J[^], [5]Nichols J, [6,7]Grozeva D, [8]Joseph AP,

5 [9]Mencacci NE, [1,10]Papandreou A, [1,10]Ng J, [1]Barral S, [1,10]Ngoh A,[11]Ben-Pazi H,

6 [12]Willemsen MA, [13]Arkadir D, [14]Barnicoat A,[15]Bergman H, [10]Bhate S, [16]Boys A,

7 [17]Darin N, [18]Foulds N, [19]Gutowski N, [20]Hills A, [9]Houlden H, [14]Hurst J, [21]Israel Z,

8 [22]Kaminska M, [23]Limousin P, [22]Lumsden D, [24]McKee S, [25,26]Misra S,

9 [25,26]Mohammed SS, [22]Nakou V, [27]Nicolai J, [28]Nilsson M, [29]Pall H, [30]Peall KJ,

10 [31]Peters GB, [10]Prabhakar P, [32]Reuter MS, [33]Rump P, [34]Segel R, [27]Sinnema M,

11 [35]Smith M, [4]Turnpenny P, [15]White S, [36]Wieczorek D, [20]Wilson B, [14]Winter G,

12 [19]Wragg C, [37]Pope S, [37,38]Heales SJH, [39]Morrogh D, [7]The UK10K Consortium,

13 [40]DDD study, [3]NIHR Bioresource Rare Diseases Consortium, [9]Pittman A, [10]Carr LJ,

14 [41,42]Perez-Dueñas B, [22]Lin JP, [32]Reis A, [43]Gahl WA, [43]Toro C, [9,23]Bhatia KB,

15 [9,23]Wood NW, [44]Kamsteeg EJ, [45]Chong WK, [5]Gissen P, [8]Topf M, [25,26]Dale RC,

16 [5]Chubb JR, [3,6,7]Raymond FL[+], [1,10]Kurian MA[+][*]

17
18 [^]These authors contributed equally

19 [+]These authors contributed equally
20
21

22 *Corresponding author**: Dr Manju Kurian** (manju.kurian@ucl.ac.uk)

23

24 **Affiliations:**

25 1. Molecular Neurosciences, Developmental Neurosciences, UCL-Institute of

26 Child Health, London, UK

2. Department of Haematology, University of Cambridge, NHS Blood and Transplant Centre, Cambridge, UK

3. NIHR Bioresource Rare Diseases, University of Cambridge, Cambridge, UK

4. Clinical Genetics, Royal Devon & Exeter Hospital, Exeter, UK

5. MRC Laboratory for Molecular Cell Biology, UCL, London, UK

6. Department of Medical Genetics, Cambridge Institute for Medical Research, University of Cambridge, Cambridge, UK

7. Wellcome Trust Sanger Institute, Hinxton, Cambridge, UK

8. Institute of Structural and Molecular Biology, Crystallography/Department of Biological Sciences, Birkbeck College, University of London, London, UK

9. Department of Molecular Neuroscience, UCL-Institute of Neurology, London, UK

10. Department of Neurology, Great Ormond Street Hospital, London, UK

11. Pediatric Neurology and Development, Shaare-Zedek Hospital, Jerusalem, Israel

12. Department of Paediatric Neurology, Donders Centre for Brain, Cognition, and Behavior, Radboud University Medical Center, Nijmegen, Netherlands

13. Department of Neurology, Hadassah Medical Center and the Hebrew University, Jerusalem, Israel

14. Department of Clinical Genetics, Great Ormond Street Hospital, London, UK

15. Department of Neurobiology and Neurosurgery, The Hebrew University, Hadassah Medical Centre, Jerusalem, Israel

16. Victoria Clinical Genetics Services, Murdoch Children's Research Institute, Parkville, Victoria, Australia

51   17. Department of Neurology, The Queen Silvia Children´s Hospital,
52   Sahlgrenska University Hospital, Gothenburg, Sweden

53   18. Department of Clinical Genetics, Southampton General Hospital,
54   Southampton, UK

55   19. Department of Neurology, Royal Devon and Exeter NHS Foundation Trust,
56   Exeter, UK

57   20. Bristol Genetics Laboratory, Bristol, UK

58   21. Functional and Restorative Neurosurgery, Hadassah University Hospital,
59   Jerusalem, Israel

60   22. Complex Motor Disorders Service, Evelina Children's Hospital, Guy's & St
61   Thomas' NHS Foundation Trust, London, UK

62   23. Sobell Department of Motor Neuroscience and Movement Disorders,
63   National Hospital for Neurology and Neurosurgery, London, UK

64   24. Northern Ireland Regional Genetics Service, Belfast City Hospital, Belfast,
65   UK

66   25. Child and Adolescent Health, University of Sydney, Sydney, Australia

67   26. Institute for Neuroscience and Muscle Research, The Children's Hospital at
68   Westmead, University of Sydney, Sydney, Australia

69   27. Department of Neurology, Maastricht University Medical Center, Netherlands

70   28. Department of Pediatrics, Piteå Hospital & Umeå University Hospital,
71   Sweden

72   29. College of Medicine and Dental Studies, The University of Birmingham,
73   Birmingham, UK

74 30. Neuroscience and Mental Health Research Institute, Institute of
75   Psychological Medicine and Clinical Neurosciences, Cardiff University,
76   Cardiff, UK

77 31. Department of Cytogenetics, The Children's Hospital at Westmead,
78   Westmead, Australia

79 32. Institute of Human Genetics, Friedrich-Alexander-Universität Erlangen-
80   Nürnberg, Erlangen, Germany

81 33. Department of Genetics, University of Groningen, University Medical Center
82   Groningen, Netherlands

83 34. Medical Genetics Institute and Pediatrics, Shaare Zedek Medical Center and
84   the Hebrew University School of Medicine, Jerusalem, Israel

85 35. Department of Paediatric Neurology, John Radcliffe Hospital, Oxford, UK

86 36. Institute of Human Genetics, University Duisburg-Essen, Essen, Germany

87 37. Neurometabolic Unit, National Hospital for Neurology and Neurosurgery,
88   Queen Square, London, UK

89 38. Clinical Chemistry, Great Ormond Street Children's Hospital, NHS
90   Foundation Trust, London, UK

91 39. North East Thames Regional Genetics Service, Great Ormond Street
92   Hospital, London, UK

93 40. DDD Study, Wellcome Trust Sanger Institute, Hinxton, Cambridge, UK

94 41. Department of Child Neurology, Hospital Sant Joan de Déu, Universitat de
95   Barcelona, Barcelona, Spain

96 42. Centre for Biomedical Research in Rare Diseases (CIBERER-ISCIII),
97   Hospital Sant Joan de Déu, Barcelona, Spain

98 43. NIH Undiagnosed Diseases Program, Common Fund, Office of the Director,

99   National Institutes of Health, Bethesda, Maryland, USA

100   44. Department of Human Genetics, Radboud University Medical Center,

101   Nijmegen, Netherlands

102   45. Department of Radiology, Great Ormond Street Hospital, London, UK

103 **ABSTRACT**

104 Histone lysine methylation mediated by mixed-lineage leukemia (MLL) proteins, has

105 emerged as critical in the regulation of gene expression, genomic stability, cell cycle

106 and nuclear architecture. Although postulated to be essential for normal

107 development, little is known about the specific functions of the different MLL lysine

108 methyltransferases. Here, we report heterozygous mutations in *KMT2B (MLL4)* in

109 27 unrelated individuals with a complex progressive childhood-onset dystonia, often

110 associated with a typical facial appearance and characteristic findings on brain

111 magnetic resonance imaging. Over time the majority developed prominent cervical,

112 cranial and laryngeal dystonia. Marked clinical benefit was observed following deep

113 brain stimulation (DBS), leading to even restoration of independent ambulation in

114 some cases. Decreased gene expression of *THAP1* and *TOR1A* was evident in

115 cultured skin fibroblasts from subjects with *KMT2B* mutations, with reduced THAP1

116 protein levels on immunoblotting. Analysis of cerebrospinal fluid from *KMT2B*

117 mutation-positive patients revealed markedly reduced levels of dopamine 2 receptor

118 protein, with increased tyrosine hydroxylase levels. Our findings highlight a major

119 new, clinically recognizable, and potentially treatable form of genetic dystonia,

120 demonstrating the crucial role of KMT2B in the physiological control of voluntary

121 movement.

122

INTRODUCTION

124 The control of voluntary movement is governed by interactive neural networks

125 within the brain, involving the basal ganglia, sensorimotor cortex, cerebellum and

126 thalamus[1]. Disruption of such pathways can lead to the development of a variety of

127 motor disorders. Dystonia is one such movement disorder characterized by

128 sustained or intermittent muscle contractions, causing abnormal, often repetitive

129 movements and postures affecting the limbs, trunk, neck and face. Dystonic

130 movements are typically patterned, twisting, and may be tremulous, often initiated

131 or worsened by voluntary action and associated with overflow muscle activation[2].

132 Dystonia is the 3rd most commonly reported movement disorder worldwide[1]. It is

133 described in a broad spectrum of genetic and acquired disorders, either in isolation

134 or combined with other neurological and systemic features[2]. The precise

135 pathophysiological processes remain yet to be fully elucidated, but defective

136 dopaminergic signaling is thought to play an important role in many forms of

137 isolated and complex dystonia[1,3-5].

138 Despite genetic advances, the underlying cause remains elusive for a significant

139 proportion of individuals with childhood-onset dystonia, hindering future

140 prognostication and treatment strategies[6]. Here we report 27 individuals with an

141 early-onset, complex, combined progressive dystonia associated with mono-allelic

142 mutations in *KMT2B* (*MLL4*, OMIM *606834). *KMT2B* encodes a lysine histone

143 methyltransferase, involved in H3K4 methylation, an important epigenetic

144 modification associated with active gene transcription.

145

RESULTS

Chromosomal microdeletions and intragenic KMT2B mutations in early-onset dystonia

We identified a cohort of 34 patients with undiagnosed childhood-onset dystonia for further molecular genetic investigation ([**Online Methods, Supplementary Table 1**, **Supplementary Fig. 1**). On routine diagnostic testing, one case (Patient 1) was found to have a microdeletion at 19q13.12 of undetermined significance[7]. Diagnostic chromosomal microarray was therefore undertaken in as many patients as logistically possible from this cohort (n=20) and overlapping microdeletions were detected in 5 more children (**Supplementary Table 1**, Patients 2-6). Using established networks (**Online Methods, Supplementary Fig. 1**), 4 more cases (Patients 7-10) with microdeletions were identified. In total, 10 patients (Patients 1-10) were found to have overlapping heterozygous interstitial microdeletions at 19q13.11-19q13.12 (**Table 1a, Fig.1**). Deletions detected on diagnostic microarray studies were confirmed by standard established laboratory protocols and confirmed *de novo* where parental testing was possible (**Supplementary Table 2a**). The smallest region of overlap extended from 36,191,100-36,229,548bp (GRCh37/Hg19), and contained two HUGO Gene Nomenclature Committee curated genes, *ZBTB32* (zinc finger and BTB domain containing 32) and *KMT2B* (*MLL4*) (**Fig. 1**).

Of the remaining 28 patients from the original cohort, we undertook research exome (n=6) and genome sequencing (n=9) in 15 patients (**Online Methods**). Heterozygous variants of *KMT2B* were identified in 6/15 cases (Patients 13, 14, 17,

169   21, 22, 27). Subsequent Sanger sequencing of *KMT2B* in the other 13/28

170   individuals from the original cohort detected one more mutation-positive case

171   (Patient 16). A further 10 cases (Patients 11, 12, 15, 18, 19, 20, 23, 24, 25, 26a)

172   were ascertained through both national and international collaborators (**Online**

173   **Methods, Supplementary Fig. 1**). In total, 17 patients with intragenic heterozygous

174   *KMT2B* variants were identified, harboring frameshift insertions (n=1), frameshift

175   deletions (n=6), splice site (n=1), stop-gain (n=2) and missense (n=7) mutations

176   (**Fig.1**). All *KMT2B* mutations were confirmed on Sanger sequencing and parental

177   segregation studies completed where DNA was available (**Table 1a, Fig. 1,**

178   **Supplementary Table 2a, Supplementary Fig. 2**). No pathogenic variants in

179   either *ZBTB32* or other known disease-associated genes (including genes causing

180   clinically similar forms of dystonia) were otherwise identified in patients who had

181   whole exome or genome sequencing. In the remaining patients, where further

182   genetic testing was possible, mutations in *TOR1A, THAP1 and GNAL* were

183   excluded by diagnostic single gene testing, multiple gene panel testing or research

184   Sanger sequencing (**Supplementary Table 3**).

185   ***Phenotypic characterization of patients with KMT2B mutations***

186   Overall, we identified 27 patients (current age 6-40 years, 14 female, 13 male) with

187   childhood-onset progressive dystonia (**Table 1a, Table 1b, Supplementary Table**

188   **4, Supplementary Videos 1-7**). Individuals presented in early childhood (1-9 years,

189   median age 4 years) with either limb or cranio-cervical dystonia. Clinical

190   presentation for those with microdeletions, frameshift, splice-site and stop-gain

191   variants (mean age 4.1 years) occured significantly earlier than for those with

192   intragenic missense mutations (mean age 6.4 years) (p-value 0.0223)

193   (**Supplementary Fig. 3a**). Most patients (21/27) had lower limb symptoms at

194   disease onset, leading to foot posturing, toe-walking and gait disturbance (**Fig. 2a**).

195   4/27 patients presented initially with upper limb symptoms associated with

196   abnormal postures (**Fig. 2b,c**) and dystonic tremor, leading to reduced dexterity

197   and handwriting difficulties (**Supplementary Fig. 4a,b**). With increasing age,

198   cervical symptoms (torticollis, retrocollis) (**Fig. 2d,e**) and cranial involvement (facial

199   dystonia, oromandibular involvement with dysarthria/anarthria and difficulties in

200   chewing/swallowing) became prominent features in the majority of patients. In many

201   patients, progressively severe dysphonia was suggestive of laryngeal involvement.

202   None of the patients had airway compromise and videostroboscopy was not

203   undertaken. Over time, the majority of patients (24/27) developed progressive

204   generalized dystonia, 2-11 years after initial presentation (**Fig. 2f**). The dystonia

205   was persistent in nature, absent in sleep, worsened by voluntary action and

206   associated with overflow muscle activation. Some patients had dystonic tremor.

207   Sudden, brief, involuntary muscle jerks, clinically consistent with myoclonus was

208   evident in 2 cases (Patients 14 and 27). For a few subjects, dystonia was

209   exacerbated when systemically unwell. Stepwise deterioration following intercurrent

210   illness was particularly evident in Patient 14, and status dystonicus, triggered by a

211   urinary tract infection, was reported in Patient 3.

212   Many patients with *KMT2B* mutations had further clinical findings. Additional

213   neurological symptoms and signs were evident in some patients, including

214   microcephaly, seizures, spasticity and eye movement abnormalities (strabismus,

215   saccade initiation failure and oculomotor apraxia) (**Table 1b**). Dysmorphic features

216   and characteristic facial appearance (elongated face and bulbous nasal tip) (**Fig.**

217   **2g, Table 1b**) were commonly reported. Delay in neurodevelopmental milestones,

218 intellectual disability, systemic (dermatological, renal, respiratory) features and

219 psychiatric symptoms were also present in some individuals (**Table 1b,**

220 **Supplementary Table 4, Supplementary Fig. 4c**). Malignancies were not reported

221 in any patients. Cerebrospinal fluid (CSF) neurotransmitter analysis was undertaken

222 in 13 patients revealing no major derangement of monoamine metabolites

223 (**Supplementary Table 5a**). Magnetic resonance (MR) imaging revealed a

224 characteristic signature in 17/22 patients who had imaging sequences suitable for

225 assessment (**Supplementary Table 5b**). Subtle symmetrical hypointensity of the

226 globus pallidi (with a hypointense streak of bilateral globus pallidus externa) was

227 evident on MR images known to be sensitive to the magnetic resonance

228 phenomenon of susceptibility (T2*-, susceptibility- and echo-planar imaging b0-

229 diffusion-imaging datasets) (**Fig. 3**)**.** The mean age at neuroimaging was

230 significantly lower for patients with MR abnormalities (11.7 years) than for those

231 with normal brain scans (19.0 years) (p-value 0.0167) (**Supplementary Fig. 3b**).

232 Single positron emission tomography using [123]I (DaTSCAN[TM]) and 18 FDG-PET-CT

233 glucose uptake studies, each undertaken in 3 patients, were normal

234 (**Supplementary Table 5b, Supplementary Fig. 4d**).

235 ***Deep brain stimulation: clinical benefit in KMT2B-dystonia***

236 Overall, medical therapies were not of clinical benefit in this patient cohort. None of

237 the patients had a sustained response to levodopa treatment, nor other commonly

238 used anti-dystonic agents (**Table 1a**). Due to the medically intractable, progressive

239 nature of disease, 10 patients had symptomatic treatment with bilateral globus

240 pallidus interna-deep brain stimulation (GPi-DBS) (**Table 1a**). All showed clinical

241 benefit with DBS (which was particularly striking in some of the younger patients)

242 with overall amelioration of dystonia, improved oromandibular symptoms, better

243 upper and lower limb function and even restoration of independent ambulation in

244 some patients. Patient 6 showed significant improvement of torticollis and

245 retrocollis, as well as in overall function and gait after DBS. Patient 8 showed a

246 sustained clinical response 6 years after DBS insertion, with improvement of

247 dystonia, even more evident after replacement of a faulty right DBS lead. Patient 9

248 had generalized dystonia and could not walk independently pre-DBS. Two weeks

249 post-DBS insertion he dramatically regained independent ambulation with marked

250 improvement of dystonic symptoms (**Supplementary Video 8**). Patient 17 and 21

251 were predominantly wheelchair-dependent pre-DBS insertion, but both patients

252 showed restoration of independent walking and improvement of dystonia after DBS

253 (**Supplementary Video 9,10**). Patient 19 had improvement in oromandibular

254 symptoms with DBS. Patient 20 had DBS insertion at age 32 years and although

255 most benefits were only transient, sustained improvement of foot posture was

256 reported. Patient 23 had significant amelioration of dystonia symptoms after DBS

257 insertion. Patient 22, now 9 months post-DBS (**Supplementary Video 11**) and

258 Patient 25, 4 months post-DBS have both shown significant gains in hand function

259 and independent walking with reduction of dystonia. Five patients in the cohort are

260 now over three years post-surgery, and the observed reduction of dystonia,

261 restoration of function and prevention of progressive disability is evidence of

262 sustained clinical benefit.

263 ***KMT2B is constrained for missense and predicted protein truncating variants***

264 Four individuals (Patient 13, 14, 17 and 21) had whole genome sequencing as part

265 of the NIHR-funded BioResource-Rare Disease project. Enrichment analysis was

266 undertaken in this cohort in order to determine whether predicted protein truncating

267   variants (PPTVs) in *KMT2B* are observed more frequently in patients than would be

268   expected by chance. Given the size and sequence context of *KMT2B*, 5.73×10^{-03} *de*

269   *novo* PPTVs are expected to occur by chance in *KMT2B* in the subset of the NIHR

270   BioResource- Rare Diseases cohort who have pediatric onset neurological disease,

271   but 3 PPTVs are observed. This represents a significant enrichment (p-value

272   3.12×10^{-08}). Furthermore in ExAC, *KMT2B* is also highly constrained for PPTVs. In

273   the ExAC database of 60,706 individuals (Exome Aggregation Consortium (ExAC),

274   Cambridge, MA (URL: http://exac.broadinstitute.org, accessed July 2016)[8], there

275   are only 5 PPTVs that are not flagged as having dubious variant annotation. All are

276   extremely rare (4 are found in a single individual and one occurs in 2 individuals).

277   Given the size and sequence context of the gene, the presence of so few PPTVs in

278   a cohort of 60,706 individuals reveals *KMT2B* to be highly constrained for such

279   variation, providing supportive evidence of its pathogenicity. Regarding variants in

280   the ExAC database, there are 712 reported non-synonymous changes. Most of

281   these are rare, as expected for a cohort of this size, and the median CADD score[9]

282   for these variants is 22.9. The median CADD score for missense mutations

283   identified in our KMT2B-dystonia cohort is significantly higher at 29.1 (p-value

284   0.0001364; **Supplementary Table 2b**). Furthermore, given the size and sequence

285   context of *KMT2B*, 956 missense variants are predicted to occur by chance,

286   suggesting that *KMT2B* may also be constrained for missense variation (z=4.06)[8].

287   ***KMT2B variants are predicted to destabilize protein structure***

288   *In silico* homology modelling studies were undertaken to generate hypotheses

289   regarding the predicted effects of mutations on KMT2B structure-function properties

290   (**Supplementary Results**). Based on Pfam domain assignments, KMT2B has a

291   CXXC zinc finger domain, multiple PHD domains, an F/Y rich N-terminus (FYRN),

292   FYRC (F/Y rich N-terminus) domain and a C-terminal SET domain (**Fig. 4a**). The

293   modelled mutations occurred in residues within the PHD-like, FYRN, SET and

294   FYRC-SET linking domains (**Fig. 4b-d**). Evaluation of a number of mutations using

295   MAESTRO[10] and DUET[11] suggests change in free energy, with a predicted

296   structure destabilizing effect (**Supplementary Results**).

297   Mutations Phe1662Leu and Gly1652Asp occur within a PHD-like domain (residues

298   1574-1688), predicted to facilitate interaction with DNA, protein-protein interaction

299   and recognition of methylated/unmethylated lysines[12-14]. Extensive hydrophobic

300   interactions hold the globular structure of this region, which is important for its

301   function[12]. Phe1662 is fully buried at the core, stabilizing the structure of this PHD-

302   like domain while Gly1652 is partially buried (**Fig. 4b,e,f**). Phe1662 is involved in

303   multiple hydrophobic contacts at the core of the PHD domain, and mutation to

304   leucine is predicted to cause loss of contacts at the core (**Fig. 4g**). Gly1652 is

305   located on a loop (**Fig. 4e**) and mutation to aspartic acid is predicted to alter surface

306   charge, with possible effect on the interaction network in the vicinity, involving a

307   positively charged Arg1635, part of the helix α3 implicated in DNA binding[12].

308   Arg1762 and Leu1781 occur in a FYRN domain. FYRN and FYRC regions,

309   particularly common in MLL histone methyltransferases, interact to form a compact

310   structural unit (**Fig. 4c,h**), important in maintaining the active structure[15,16]. Arg1762

311   forms hydrogen bonds with the backbone carboxyls of Arg2463 and Leu2464 of

312   FYRC domain. Substitution of Arg1762 by cysteine is predicted to abolish these

313   contacts and hence contribute to destabilization of FYRC-FYRN association.

314   Leu1781, at the interface between FYRN and FYRC (**Fig. 4h,i**) is surface exposed

315   and involved in backbone hydrogen bonds stabilizing the beta sheet formed

316 together by the two domains. Mutation to proline is predicted to disrupt the

317 backbone hydrogen bond at this position, because it lacks one hydrogen bond

318 donor and its backbone torsion angles are not compatible with that of a beta sheet,

319 with a predicted destabilizing effect on sheet structure, potentially affecting the

320 normal association of FYRN and FYRC domains. Arg2517 resides in the region

321 linking FYRC and SET domains, known to bind WDR5, an effector required for

322 trimethylation of histone H3[17], presenting methylated histone H3 substrates to the

323 MLL complex for further methylation[18]. Arg2517 is thought to be involved in a salt-

324 bridge interaction with Asp172 of WDR5 (**Fig. 4j**) and Arg2517Trp is predicted to

325 lead to loss of this interaction. Ile2674, Tyr2688 and Ile2694 occur in the catalytic

326 methyltransferase SET domain common to histone lysine methyltransferases.

327 Ile2674 is buried in the hydrophobic core, adjacent to the catalytic site (**Fig. 4d,k**).

328 Mutation to threonine is predicted to lead to loss of contacts at the core of the

329 domain (due to the shorter side chain) and also introduces a buried polar group

330 (**Fig. 4k,l**). Tyr2688Thr occurs at the core of SET domain involving extensive

331 hydrophobic interactions and a hydrogen bond interaction with Ser2661 (**Fig 4m**).

332 The frameshift mutation Tyr2688Thrfs*50 with insertion of 50 additional residues, is

333 predicted to destabilise the core and affect contacts due to the substitution with a

334 shorter non-aromatic side-chain. Ile2694 is involved in the extensive hydrophobic

335 contacts stabilizing the core of this domain. *In silico* analysis predicts that the

336 frameshift mutation Ile2694Serfs*44 will disrupt the domain fold and affect

337 methytransferase activity.

338 **KMT2B is ubiquitously expressed with reduced expression in KMT2B-**

339 **dystonia**

340   We confirmed widespread *KMT2B* expression in a variety of control fetal and adult

341   human tissues (**Fig. 5a**). Moreover, *KMT2B* is ubiquitously expressed in the brain,

342   with higher expression in the cerebellum than any other region (**Fig. 5b**). We

343   ascertained fibroblasts from 4 patients (Patient 2, 13, 14, 16, with either

344   microdeletions or PPTVs in *KMT2B*) and detected a statistically significant

345   decrease in fibroblast *KMT2B* expression on quantitative RT-PCR when compared

346   to control fibroblasts (**Fig. 5c**).

347   ***Histone H3K4 methylation is not globally reduced in KMT2B-dystonia***

348   To determine the effect of *KMT2B* mutations on methylation of lysine 4 on histone

349   H3 (H3K4 methylation), we assayed tri-methylated H3K4 (H3K4me3) and di-

350   methylated H3K4 (H3K4me2). Immunoblotting of histones extracted from fibroblasts

351   of Patient 14 and 16 showed no significant reduction in H3K4me3 or H3K4me2

352   relative to control samples (**Fig. 5d, Supplementary Fig. S5a**). We used the model

353   species *Dictyostelium discoideum* to test the effect of SET domain mutation

354   Ile2647Thr on *in vivo* histone methyltransferase activity. The SET domain of

355   KMT2B shares 56**%** sequence identity with the *Dictyostelium* orthologue DdSet1,

356   and Ile2647 is conserved (corresponding amino acid in *Dictyostelium* is Ile1447)

357   (**Fig. 1h**). DdSet1 is the only H3K4 methyltransferase in *Dictyostelium* and targeted

358   knockout of *DdSet1* (*set1⁻*) results in loss of all methylation at H3K4[19]. We

359   constitutively expressed wild-type DdSet1 (WT-DdSet1) and mutant-DdSet1 (m-

360   DdSet1), both with N-terminal GFP fusions, in *set1- Dictyostelium* cells and

361   compared the resulting levels of H3K4 methylation. Expression of either GFP-WT-

362   DdSet1 or GFP-mDdSet1 in *set1-* cells resulted in rescue of H3K4 tri-methylation to

363   wild type levels (**Fig. 5e, Supplementary Fig. S5b, S5c**).

364   ***Fibroblast THAP1 gene and protein expression is reduced in KMT2B-dystonia***

365   In order to determine whether KMT2B-dystonia is associated with dysregulation of

366   specific genes implicated in the control of movement, we investigated the

367   expression profiles of *TOR1A* and *THAP1.* Fibroblasts derived from 4 patients

368   (Patients 2, 13, 14, 16) showed significantly reduced transcript levels of *THAP1* and

369   *TOR1A* when compared to control fibroblasts (**Fig. 5f**). Fibroblast immunoblotting

370   studies showed a statistically significant reduction in THAP1 protein expression in

371   all 4 patients when compared to control samples (**Fig. 5g**). A statistically significant

372   reduction in TOR1A protein level was evident in Patient 14, though not in the other

373   patients (**Fig. 5h**).

374   ***Abnormal CSF levels of dopaminergic proteins in KMT2B-dystonia***

375   CSF immunoblotting studies were undertaken in two patients for whom samples

376   were available for research testing (Patient 2 and 16). Both patients had markedly

377   reduced levels of dopamine 2 receptor (D2R), 56.9% and 59.8% of levels observed

378   in control CSF (Controls = 1.09±0.21SD, KMT2B patients = 0.64±0.02SD). In

379   contrast, an increase in tyrosine hydroxylase (TH) levels was seen in both mutation-

380   positive patients (173.3% and 170.9% of levels seen in control CSF) (Controls =

381   0.52±0.08SD, KMT2B patients = 0.90±0.01SD) (**Fig. 5i**).

382   # DISCUSSION

383   We report 27 individuals with heterozygous mutations in the lysine

384   methyltransferase gene, *KMT2B,* and define a new genetic movement disorder that

385   importantly, is amenable to treatment with DBS*.* Using the current classification

386   system[2], KMT2B-dystonia is defined as an inherited autosomal dominant, complex,

387 combined dystonia usually of infantile or childhood-onset. In most patients, the

388 dystonia is persistent and progressive in nature. The majority of individuals develop

389 4-limb dystonia with particularly prominent cervical, laryngeal and oromandibular

390 symptoms. Whilst the majority of patients in this cohort seem to follow this disease

391 trajectory, we also report atypical cases with relatively little limb involvement and

392 either mainly oromanibular features (Patient 18) or paroxysmal cervical dystonia

393 (Patient 26a).

394 For many patients, KMT2B-dystonia is associated with a number of additional

395 clinical features, including other neurological symptoms, intellectual disability,

396 psychiatric co-morbidity, dysmorphia, skin lesions and other systemic signs. Given

397 the association with active gene expression, is possible that *KMT2B* could account

398 for these additional disease features. For Patients 1-10, is also possible that other

399 genes within their microdeletion could contribute to aspects of their clinical

400 phenotype. Indeed, cutis aplasia and ectodermal dysplasia have been reported in

401 patients with more proximal deletions of chromosome 19q13.11[20]. KMT2B is

402 therefore a complex dystonia, and affected patients should have close surveillance

403 of development during childhood, regular neurology assessments, routine

404 dermatological review and formal neuropsychiatric testing.

405 In KMT2B-dystonia, the majority of patients had a characteristic pattern on MR

406 imaging, with very subtle low pallidal signal on T2*-, diffusion- and susceptibility-

407 weighted sequences, particularly affecting the lateral aspect of the globus pallidus

408 externa (**Fig. 3**). Although genotype did not appear to influence whether MR

409 findings were evident, those with abnormal imaging had scans undertaken at a

410 significantly younger age than those with normal imaging. Indeed, MR abnormalities

411 could possibly be an age-dependent phenomenon, perhaps becoming less

412   apparent with increasing age, as was evident in Patient 22 (**Supplementary Table**

413   **5b, Supplementary Fig. 3b,c,d**). The overall significance of the identified

414   neuroradiological abnormalities remains unclear. Such radiological findings are

415   reminiscent of, but much more subtle and different to those reported in classical

416   Neurodegeneration with Brain Iron Accumulation (NBIA) syndromes[21,22]. Similar

417   non-specific features of T2*-weighted hypointensity are increasingly recognized in a

418   number of other neurological conditions, including Huntington's disease, *TUBB4A*-

419   related   disorders,   GM1   gangliosidosis,   alpha-fucosidosis   and

420   mitochondriocytopathies.

421   In the original UCL-ICH Dystonia cohort, *KMT2B* mutations were identified in 13/34

422   (38%) individuals with a relatively homogenous phenotype of early onset

423   progressive dystonia. In other screened cohorts, mutation detection rates varied

424   from 1.3-30%, with more cases identified from cohorts that were tightly phenotyped

425   for dystonia (**Supplementary Fig. 1**). In screened cases where *KMT2B* mutations

426   were not detected, it is likely that these individuals have another underlying etiology

427   accounting for their symptoms, although it is possible that (i) single/multiple exon

428   *KMT2B* deletions and duplications may have been missed on microarray, Sanger

429   sequencing and whole exome/genome sequencing and (ii) promoter mutations and

430   deeply intronic *KMT2B* variants may not have been detected by whole exome and

431   Sanger sequencing.

432   The majority of individuals with *KMT2B* mutations (20/27, Patients 1-20) had either

433   heterozygous interstitial microdeletions leading to *KMT2B* haploinsufficiency, or

434   variants predicted to cause protein truncation, protein elongation, splicing defects or

435   nonsense-mediated mRNA decay. The remaining 7 patients (Patients 21-27) had

436   previously unreported non-synonymous variants of *KMT2B*, all affecting conserved

437 residues within key protein domains (**Fig. 1c-h**), and *in silico* studies predict

438 destabilization of protein structure. Notably, initial disease presentation was

439 significantly earlier in Patients 1-20 than in those with missense variants

440 (**Supplementary Fig. 3a**). In KMT2B-dystonia, genotype did not however influence

441 the rate of symptom evolution, disease severity or response to DBS.

442 For the majority of patients, *KMT2B* mutations were confirmed as *de novo* where

443 parental testing could be undertaken. In our cohort, 3 patients had missense

444 mutations that were all maternally inherited (Patient 22, 26a, 27). Given this

445 observation of maternal inheritance, the possibility of imprinting at the disease locus

446 was considered, but deemed unlikely, given (i) *de novo* microdeletions in Patients 2

447 and 10 occurred on paternally inherited alleles and (ii) there is evidence of bi-allelic

448 expression of *KMT2B* single nucleotide polymorphisms in human tissues, including

449 brain (**Supplementary Fig. S6**). Importantly, whole exome sequence analysis

450 undertaken in Patients 22, 26a and 27 did not identify other rare or *de novo* variants

451 to account for their disease. Interestingly, Patient 26a inherited p.Arg2517Trp from

452 his symptomatic mother (26b) who also had (milder) disease symptoms. She

453 reported gait abnormalities and a progressive inability to run, as well as periodic

454 paroxysmal upper limb and neck dystonia. She also had a bulbous nasal tip, like

455 her son (**Fig. 2g**). In contrast, both mothers of Patients 22 and 27 were clinically

456 examined, and neither had evidence of a motor phenotype, intellectual disability,

457 other neurological features, neuropsychiatric symptoms, facial dysmorphia, skin

458 lesions or other systemic signs. The identification of both symptomatic and

459 asymptomatic carriers suggests that there may be either "apparent' incomplete

460 penetrance, due to parental mosaicism, or true incomplete disease penetrance, a

461 phenomenon commonly reported in a number of other autosomal dominant genetic

462 dystonias[23,24]. Furthermore, other genetic, epigenetic and environmental modifiers

463 may also influence disease penetrance and phenotypic presentation in KMT2B-

464 dystonia.

465 *KMT2B* encodes an ubiquitously expressed lysine methyltransferase specifically

466 involved in H3K4 methylation[25,26], an important epigenetic modification associated

467 with active transcription. H3K4me3 is enriched at promoters, marking transcription

468 start sites of actively transcribed genes, whereas H3K4me1 is associated with

469 active enhancer sequences[27]. H3K4me2 is less specifically localized, but may be

470 enriched at transcription factor binding sites[28]. Members of the SET/MLL protein

471 family, including KMT2B, are responsible for the generation of H3K4me1,

472 H3K4me2, and H3K4me3, essential for gene activation in normal development[29].

473 Using patient-derived fibroblasts and a *Dictyostelium discoideum* model, we

474 demonstrated that *KMT2B* mutations are not associated with widespread alterations

475 in overall levels of H3K4 methylation. This is not surprising, given that

476 haploinsufficiency of other MLL family members have not been convincingly shown

477 to affect global H3K4 levels. The fundamental physiological role of MLL proteins is

478 however further affirmed by the observation that loss-of-function heterozygous

479 mutations in MLL-encoding genes are reported in human developmental

480 disorders[30], namely Wiedemann Steiner (*KMT2A, MLL1*)[31], Kleefstra-like (*KMT2C,*

481 *MLL3*)[32], Kabuki (*KMT2D, MLL2*)[33] syndrome, and most recently *SETD1A*-related

482 disease (*KMT2F*)[34]. The physiological functions of MLL proteins are yet to be fully

483 characterized, however, the observation that mutations in different MLL genes

484 cause phenotypically distinct syndromes (**Supplementary Table 6**) suggests that

485 each MLL protein has a unique role regulating the expression of a specific set of

486 genes[35,36].

487   Amongst the 4 reported *MLL*-gene disorders, dystonia appears unique to KMT2B-

488   related disease and is not described in other MLL syndromes (**Supplementary**

489   **Table 6**), providing further evidence that different MLL proteins mediate the

490   activation and transcription of a specific set of genes, with temporal and cellular

491   context[37]. We utilized fibroblasts and CSF derived from patients to investigate

492   downstream effects of *KMT2B* mutations on specific gene expression. The rationale

493   for investigating *THAP1* and *TOR1A* in the first instance was based on a number of

494   factors, namely that (i) loss-of-function mutations in both genes cause progressive

495   generalized dystonia with cervical, oromandibular and laryngeal symptoms, similar

496   to those seen in KMT2B-dystonia[38,39,40], (ii) both genes are expressed in fibroblasts,

497   facilitating investigation in patient-derived tissue, (iii) analysis of methylation profiles

498   using ENCODE demonstrates a sharp H3K4me3 peak at the 5' region of both

499   *THAP1* and *TOR1A* in a wide range of cell types, including brain cells

500   (**Supplementary Fig. 7**), (iv) on human brain expression profiles, *THAP1* and

501   *KMT2B* similarly display highest expression in the cerebellum (**Fig 5b,**

502   **Supplementary Fig. 8**). We detected statistically significant reduced levels of

503   *THAP1* and *TOR1A* gene expression and THAP1 protein expression in patient

504   fibroblasts. The mechanisms causing such alterations in KMT2B-dystonia remain

505   yet to be elucidated. Whilst H3K4 methylation is clearly associated with the process

506   of active transcription, several studies have shown that H3K4 methylation is

507   required, not for absolute transcriptional output, but rather for transcription stability

508   or consistency[41]. Recent studies have suggested that H3K4Me is required to

509   minimize transcriptional variability between cells in a population, rather than

510   absolute expression[41,42], so the effects of *KMT2B* haploinsufficiency on

511   *THAP1/TOR1A* levels could conceivably operate via an intermediary sensitive to

512   stochastic fluctuations. Whilst our study focuses on two genes, it is highly likely that

513   dysregulation of other genes and proteins are also involved in the disease

514   pathophysiology of KMT2B-dystonia. Further studies will determine whether

515   expression profiles of other genes are affected in KMT2B-dystonia and contributory

516   to the phenotype.

517   CSF analysis is increasingly recognized as a highly useful tool for studying synaptic

518   proteins and dysregulation of the dopaminergic system[43]. In our study, CSF

519   immunoblotting studies revealed significant reduction of D2R protein and increase

520   in TH levels in patients with KMT2B-dystonia when compared to control CSF

521   samples. Downregulation of D2R could conceivably impair post-synaptic activation

522   of coupled G-proteins with subsequent downstream effects, as seen in other

523   inherited dystonias. Reduced D2R striatal availability is reported in patients with

524   DYT1 and DYT6 dystonia[44,45]. Furthermore, D2R dysfunction is described in murine

525   DYT1 models, where aberrant D2R-mediated responses are associated with

526   reduced D2R protein levels and impaired G-protein activation[46]. The observed rise

527   in CSF TH levels could be secondary to reduced pre-synaptic D2 autoreceptors[47],

528   which could conceivably impact dopamine synthesis and bioavailability.

529   Interestingly patients with KMT2B-dystonia had normal CSF levels of the stable

530   dopamine metabolite, homovanillic acid (HVA), indicating normal dopamine

531   turnover (conversion of dopamine to HVA by monoamine oxidase and catechol-o-

532   methyl transferase). Whilst CSF HVA levels accurately reflect dopamine turnover,

533   they are not always a true indicator of dopamine synthesis and bioavailability. Low

534   CSF HVA levels often correlate with low dopamine levels in patients with inherited

535   disorders of dopamine deficiency such as TH deficiency, aromatic l-amino acid

536   decarboxylase deficiency, and many inherited pterin defects[3]. However HVA levels

537   may also be normal (autosomal dominant GTP cyclohydrolase deficiency) or

538   elevated (Dopamine Transporter Deficiency Syndrome) in diseases known to be

539   associated with dopamine deficiency[3,48]. Normal HVA levels in KMT2B-dystonia

540   may therefore not reflect true dopamine levels. Indeed, the effect of *KMT2B*

541   mutations on dopamine synthesis and bioavailability remain yet to be fully

542   elucidated.

543   In conclusion, we report *KMT2B* mutations in 27 patients with a clinically

544   recognizable, distinct form of dystonia. To date, the underlying etiology is only

545   genetically resolved in a minority of childhood-onset cases of dystonia, which

546   precludes confirmatory diagnosis, accurate disease prognostication and selection of

547   appropriate treatment strategies. We have shown that many patients with molecular

548   confirmation of KMT2B-dystonia have significant, sustained clinical improvement

549   with DBS and referral for DBS assessment should thus be considered for this group

550   of individuals. Identification of additional cases will allow further characterization of

551   the full phenotypic disease spectrum. Our report highlights mutations in *KMT2B* as

552   a new and important cause of early-onset dystonia, emphasizing the crucial role of

553   KMT2B in the control of normal voluntary movement.

References

1. Charlesworth, G., Bhatia, K.P. & Wood, N.W. The genetics of dystonia: new twists in an old tale. *Brain* **136**, 2017-2037 (2013).

2. Albanese, A. *et al.* Phenomenology and classification of dystonia: a consensus update. *Mov. Disord.* **28**, 863-873 (2013).

3. Ng, J., Papandreou, A., Heales, S.J. & Kurian, M.A. Monoamine Neurotransmitter Disorders – clinical advances and future perspectives. *Nat. Rev. Neurol.* **11**, 567-584 (2015).

4. Fuchs, T. *et al.* Mutations in GNAL cause primary torsion dystonia. *Nat. Genet.* **45**, 88-92 (2013).

5. Karimi, M. & Perlmutter J.S. The role of dopamine and dopaminergic pathways in dystonia: insights from neuroimaging. *Tremor Other Hyperkinet. Mov.* **5**, 280 (2015).

6. Lin, J.P., Lumsden, D.E., Gimeno, H. & Kaminska, M. The impact and prognosis for dystonia in childhood including dystonic cerebral palsy: a clinical and demographic tertiary cohort study. *J. Neurol. Neurosurg. Psychiatry* **85**, 1239-1244 (2014).

7. Dale, R.C., Grattan-Smith, P., Nicholson, M. & Peters, G.B. Microdeletions detected using chromosome microarray in children with suspected genetic movement disorders: a single-centre study. *Dev. Med. Child Neurol.* **54**, 618-623 (2012).

8. Lek, M. *et al.* Analysis of protein-coding genetic variation in 60,706 humans. bioRxiv [Internet]; Available from: http://biorxiv.org/content/early/2015/10/30/030338.abstract (2015).

9. Kircher, M. *et al.* A general framework for estimating the relative

579   pathogenicity of human genetic variants. *Nat. Genet.* **46**, 310-315 (2014).

580   10. Laimer, J., Hofer, H., Fritz, M., Wegenkittl, S. & Lackner, P. MAESTRO--

581   multi agent stability prediction upon point mutations. *BMC Bioinformatics* **16**,

582   116 (2015).

583   11. Pires, D.E., Ascher, D.B. & Blundell, T.L. DUET: a server for predicting

584   effects of mutations on protein stability using an integrated computational

585   approach. *Nucleic Acids Res.* **42**, W314-319 (2014).

586   12. Liu, Z. *et al.* Structural and functional insights into the human Borjeson-

587   Forssman-Lehmann syndrome-associated protein PHF6. *J. Biol. Chem.* **289**,

588   10069-10083 (2014).

589   13. Musselman, C.A. & Kutateladze, T.G. Handpicking epigenetic marks with

590   PHD fingers. *Nucleic Acids Res.* **39**, 9061-9071 (2011).

591   14. Sanchez, R. & Zhou, M.M. The PHD finger: a versatile epigenome reader.

592   *Trends Biochem. Sci.* **36**, 364-372 (2011).

593   15. Hsieh, J.J., Ernst, P., Erdjument-Bromage, H., Tempst, P. & Korsmeyer, S.J.

594   Proteolytic cleavage of MLL generates a complex of N- and C-terminal

595   fragments that confers protein stability and subnuclear localization. *Mol. Cell.*

596   *Biol.* **23**, 186-194 (2003).

597   16. Pless, B. *et al.* The heterodimerization domains of MLL-FYRN and FYRC--

598   are potential target structures in t(4;11) leukemia. *Leukemia* **25**, 663-670

599   (2011).

600   17. Wysocka, J*. et al*. WDR5 associates with histone H3 methylated at K4 and is

601   essential for H3 K4 methylation and vertebrate development. *Cell* **121**, 859-

602   872 (2005).

603   18. Song, J.J. & Kingston, R.E. WDR5 interacts with mixed lineage leukemia

604   (MLL) protein via the histone H3-binding pocket. *J. Biol. Chem.* **283**, 35258-

605   35264 (2008).

606   19. Chubb, J.R. *et al.* Developmental timing in Dictyostelium is regulated by the

607   Set1 histone methyltransferase. *Dev. Biol.* **292**, 519-532 (2006).

608   20. Malan, V. *et al.* 19q13. 11 deletion syndrome: a novel clinically recognisable

609   genetic condition identified by array comparative genomic hybridisation. *J.*

610   *Med. Genet.* **46**, 635-664 (2009).

611   21. Kruer, M.C. *et al.* Neuroimaging features of neurodegeneration with brain

612   iron accumulation. *AJNR Am. J. Neuroradiol.* **33**, 407-414 (2012).

613   22. Meyer, E., Kurian, M.A. & Hayflick, S.J. Neurodegeneration with Brain Iron

614   Accumulation: Genetic Diversity and Pathophysiological Mechanisms. *Annu.*

615   *Rev. Genomics Hum. Genet.* **16**, 257-279 (2015).

616   23. Ozelius, L. *et al.* SourceGeneReviews® [Internet]. Seattle (WA): University of

617   Washington, Seattle; [updated 2014 Jan 02] (1993-2016).

618   24. Klein, C. *et al.* SourceGeneReviews® [Internet]. Seattle (WA): University of

619   Washington, Seattle; [updated 2014 May 1] (1993-2016).

620   25. Kouzarides, T. Chromatin modifications and their function. *Cell* **128**, 693-705

621   (2007).

622   26. Black, J.C., Van Rechem, C. & Whetstine, J.R. Histone lysine methylation

623   dynamics: establishment, regulation, and biological impact. *Mol. Cell* **48**,

624   491-507 (2012).

625   27. Creyghton, M.P. *et al.* Histone H3K27ac separates active from poised

626   enhancers and predicts developmental state. *Proc. Natl. Acad. Sci. U S A*

627   **107**, 21931-21936 (2010).

628   28. Wang, Y., Li, X. & Hu, H. H3K4me2 reliably defines transcription factor

629   binding regions in different cells. *Genomics* **103**, 222-228 (2014).

630   29. Shao, G.B. *et al.* Dynamic patterns of histone H3 lysine 4 methyltransferases

631   and demethylases during mouse preimplantation development. *In Vitro Cell*

632   *Dev. Biol. Anim.* **50**, 603-613 (2014).

633   30. Shen, E., Shulha, H., Weng, Z. & Akbarian, S. Regulation of histone H3K4

634   methylation in brain development and disease. *Philos. Trans. R. Soc. Lond.*

635   *B. Biol. Sci.* **369** (2014).

636   31. Jones, W.D. *et al.* De novo mutations in MLL cause Wiedemann-Steiner

637   syndrome. *Am. J. Hum. Genet.* **91**, 358-364 (2012).

638   32. Kleefstra, T. *et al.* Disruption of an EHMT1-associated chromatin-

639   modification module causes intellectual disability. *Am. J. Hum. Genet.* **91**,

640   73-82 (2012).

641   33. Ng, S.B. *et al.* Exome sequencing identifies MLL2 mutations as a cause of

642   Kabuki syndrome. *Nat. Genet.* **42**, 790-793 (2010).

643   34. Singh, T. *et al.* Rare loss-of-function variants in SETD1A are associated with

644   schizophrenia and developmental disorders. *Nat. Neurosci.* **19**, 571-577

645   (2016).

646   35. Micale, L. *et al.* Molecular analysis, pathogenic mechanisms, and

647   readthrough therapy on a large cohort of Kabuki syndrome patients. *Hum.*

648   *Mutat.* **35**, 841-850 (2014).

649   36. Ang, S.Y. *et al.* KMT2D regulates specific programs in heart development via

650   histone H3 lysine 4 di-methylation. *Development* **143**, 810-821 (2016).

651   37. Jakovcevski, M. *et al.* Neuronal Kmt2a/Mll1 histone methyltransferase is

652   essential for prefrontal synaptic plasticity and working memory. *J. Neurosci.*

653   **35**, 5097-5108 (2015).

654   38. Ozelius, L.J. *et al.* The early-onset torsion dystonia gene (DYT1) encodes an

655   ATP-binding protein. *Nat. Genet.* **17**, 40-48 (1997).

656   39. Fuchs, T. *et al.* Mutations in the THAP1 gene are responsible for DYT6

657   primary torsion dystonia. *Nat. Genet.* **41**, 286-288 (2009).

658   40. Bressman, S.B. *et al.* Mutations in THAP1 (DYT6) in early-onset dystonia: a

659   genetic screening study. *Lancet Neurol.* **8**, 441-446 (2009).

660   41. Benayoun BA, *et al.* H3K4me3 breadth is linked to cell identity and

661   transcriptional consistency. *Cell* **158**, 673-688 (2014).

662   42. Muramoto, T., Müller, I., Thomas, G. Melvin, A. & Chubb, J.R. Methylation of

663   H3K4 Is required for inheritance of active transcriptional states. *Curr Biol.* **20**,

664   397-406 (2010).

665   43. Ortez, C. *et al.* Cerebrospinal fluid synaptic proteins as useful biomarkers in

666   tyrosine hydroxylase deficiency. *Mol. Genet. Metab.* **114**, 34-40 (2015).

667   44. Carbon, M. *et al.* Abnormal striatal and thalamic dopamine

668   neurotransmission: genotype-related features of dystonia. *Neurology* **72**,

669   2097-2103 (2009).

670   45. Asanuma, K. *et al.* Decreased striatal D2 receptor binding in non-manifesting

671   carriers of the DYT1 dystonia mutation. *Neurology* **64**, 347-349 (2005).

672   46. Napolitano, F. *et al.* Dopamine D2 receptor dysfunction is rescued by

673   adenosine A2A receptor antagonism in a model of DYT1 dystonia.

674   *Neurobiol. Dis.* **38**, 434-445 (2010).

675   47. Lindgren, N., *et al.* Dopamine D(2) receptors regulate tyrosine hydroxylase

676   activity and phosphorylation at Ser40 in rat striatum. *Eur. J. Neurosci.* **13**,

677   773-780 (2001).

678   48. Wijemanne, S. & Jankovic, J. Dopa-responsive dystonia--clinical and genetic

679   heterogeneity. *Nat. Rev. Neurol.* **11**, 414-424 (2015).

680   49. Trabzuni, D. *et al.* Quality control parameters on a large dataset of regionally

681   dissected human control brains for whole genome expression studies. *J.*

682   *Neurochem.* **119**, 275-282 (2011).

Acknowledgements

711   **Disclosures**

713

714 **Figure 1**

a

19 p13.3 | 19 p13.2 | 19 p13.11 | 19 q13.11 | 19 q13.2 | 19 q13.33 | 19 q13.43

32Mb · 33Mb · 34Mb · 35Mb · 36Mb · 37Mb · 38Mb · 3

Pat 1
Pat 2
Pat 3
Pat 4
Pat 5
Pat 6
Pat 7
Pat 8
Pat 9
Pat 10

ZBTB32 · KMT2B

b

▲ p.Pro134Serfs*24
■ p.Arg564*
▲ p.Glu1009Glyfs*9
▲ p.Gly1048Glufs*132
■ p.Tyr1515*
▲ p.Ala1563Aspfs*83
▲ p.Val2172Alafs*11
p.Tyr2688Thrfs*50 ▲
p.Ile2694Serfs*44 ▲

20.86 kb — Forward strand

1 2 3 4 5 6 7 8 9 10 11 12 13 14 15 16 17 18 19 20 21 22 23 24 25 26 27 28 29 30 31 32 33 34 35 36 37

c.3528+2T>A ◆
p.Gly1652Asp ●
p.Phe1662Leu ●
p.Arg1705Gln ●
p.Arg1762Cys ●
p.Leu1781Pro ●
p.Ile2674Thr ●
p.Arg2517Trp ●

c

```
Human_KMT2B     1647 PGATVGCCLSSCLSNFHFMC 1666
Dog_KMT2B       1642 PGATVGCCLSSCLSNFHFMC 1661
Cow_KMT2B       1642 PGATVGCCLSSCLSNFHFMC 1661
Mouse_Kmt2b     1653 PGATVGCCLSSCLSNFHFMC 1672
Zebrafish_kmt2ba 1454 TGATVGCCLTSCQSNYHFMC 1473
Zebrafish_kmt2bb 2147 TGATVGCCLSSCQSNYHFMC 2166
Fruit_fly_trx   1803 RGATVGCNVRSCGEHYHYPC 1822
Human_KMT2A     1942 PGATVGCCLTSCTSNYHFMC 1961
Human_PHF6       286 PGATIGCEIKACVKTYHYHC  305
                     ***:** : :* . :*:
```

d

```
Human_KMT2B     1695 VNPDGFDVLRRVYVDFEGIN 1714
Dog_KMT2B       1690 VTPDGFDVLRRVYVDFEGIN 1709
Cow_KMT2B       1699 VNPDGFDVLRRVYVDFEGIN 1718
Mouse_Kmt2b     1701 VTPDGFDVLRRVYVDFEGIN 1720
Zebrafish_kmt2ba 1501 EQGNGFEVVRRVYVDFDGIS 1520
Zebrafish_kmt2bb 2194 ITGQGFEVLRRVYVDFEGIS 2213
Fruitfly_trx    1489 TYESNFEVSRPVYVELD--- 1505
Human_KMT2A     1989 VPENGFEVFRRVFVDFEGIS 2008
                     . *:* * *:*::: **
```

e

```
Human_KMT2B     1752 RLFPIGYQCSRLYWSTVDAR 1771
Dog_KMT2B       1747 RLFPIGYQCSRLYWSTVDAR 1766
Cow_KMT2B       1756 RLFPIGYQCSRLYWSTVDAR 1775
Mouse_Kmt2b     1758 RLFPIGYQCSRLYWSTVDAR 1777
Zebrafish_kmt2ba 1558 KLYPVGYQCSRWYWSTVDPR 1577
Zebrafish_kmt2bb 2251 KLFPVGYECSRWFWSTVNPL 2270
Fruitfly_trx    1542 AVVPINFLCSRLYWSSKEPW 1561
Human_KMT2A     2046 KLFPIGYQCSRVYWSTTDAR 2065
                     : *: : *** :**: : : *
```

f

```
Human_KMT2B     1778 CRILEYRPWGPREEPAHLEA 1897
Dog_KMT2B       1773 CRILEYRPWGPREEPVHLEA 1792
Cow_KMT2B       1773 CRILEYRPWGPREEPVHLEA 1792
Mouse_Kmt2b     1784 CRILEYRPWGPREEPVHLEA 1803
Zebrafish_kmt2ba 1584 CKVSEVRPSTRCRTPSFMVD 1603
Zebrafish_kmt2bb 2277 FRVTEVRPAVQEKQVEESPD 2296
Fruit_fly_trx   1936 VRTTIQNSSST----LTALD 1951
Human_KMT2A     2072 CKIVECRPPVVEPDINSTVE 2091
                     :           .
```

g

```
Human_KMT2B     2507 HGAARAEVYLRKCTFDMFNF 2526
Dog_KMT2B       2503 HGAARAEVYLRKCTFDMFNF 2522
Cow_KMT2B       2512 HGAARAEVYLRKCTFDMFNF 2531
Mouse_Kmt2b     2514 HGAARAEVYLRKCTFDMFNF 2533
Zebrafish_kmt2ba 2655 NGCARAEVYVRKSTFDMFNF 2674
Zebrafish_kmt2bb 3563 SGCARSEVYLRKSTFDMFNF 3582
Fruitfly_trx    3155 YDCARCEPYSNRSEYDMFSW 3174
Human_KMT2A     3764 HGSARAEVHLRKSAFDMFNF 3783
                     .**.* : .:. :***.:
```

h

```
Human_KMT2B     2664 IHVEGQKHIVIFALRRILRG 2783
Dog_KMT2B       2660 IHVEGQKHIVIFALRRILRG 2679
Cow_KMT2B       2660 IHVEGQKHIVIFALRRILRG 2679
Mouse_Kmt2b     2662 IHVEGQKHIVIFALRRILRG 2681
Zebrafish_kmt2ba 2812 INVEGQKHIVIFALRKIYRG 2831
Zebrafish_kmt2bb 3721 INVEGQKHIVIFALRKIYRG 3740
Fruit_fly_trx   3677 VDILGHKHIIIFALRRIVQG 3696
Yeast_Set1      1028 IKVGGRRRIVIYALRDIAAS 1047
Dicty_Set1      1437 LTIGNQKHIIIYAKRDINIG 1456
Human_KMT2A     3921 INIDGQKHIVIFAMRKIYRG 3940
Human_SETD1A    1658 ITIESQKHIVIYSKQPIGVD 1677
Human_SETD1B    1874 ITVESQKHIVIYSKQHINVN 1893
                     : :  :::*:*:: : *
```

715
716

717

718 **Figure 1:**

719 **Molecular Genetics Findings in Patients with *KMT2B* Mutations**

720 **(a)** Top panel: Schematic representation of chromosome 19. Middle panel: Ten

721 microdeletions on 19q13.11-19q13.12 are displayed as horizontal red bars

722 (GRCh37/Hg19). Lower panel: The smallest overlapping region comprises two genes,

723 *ZBTB32* and *KMT2B*. (**b**) Schematic of exon-intron structure of *KMT2B* (based on NCBI

724 Reference Sequence: NM_014727.2) is shown indicating the location of the 7 frameshift

725 insertions and deletions (blue, above gene), 2 stop-gain mutations (dark red, above gene),

726 1 splice site variant (purple, below gene) and 7 missense changes (in green, below gene).

727 (**c**) Alignment of KMT2B amino acid sequences from seven different species, the human

728 paralog KMT2A (another member of the MLL protein family) and the human PHF6 protein

729 used to model the PHD-like domain. Gly1652 (in red) is highly conserved in all listed

730 amino acid sequences, while the Phe1662 residue (in red) is either conserved or tolerates

731 replacement by the similar amino acid, Tyr without predicted functional effect

732 (**Supplementary Fig. 10**). (**d-g**) Alignment of KMT2B amino acid sequences from seven

733 different species and the human paralog KMT2A. (**d**) Arg1705 (in red) is conserved to

734 zebrafish and in human KMT2A. (**e**) Arg1762 is fully conserved throughout species. (**f**)

735 Leu1781 (in red) is conserved in all listed mammalian homologs of KMT2B. (**g**) Arg2517

736 (in red) is conserved to zebrafish and in human KMT2A. (**h**) Alignment of KMT2B amino

737 acid sequences from seven different species, the human paralog KMT2A and SET domain

738 containing proteins (human SETD1A/SETD1B, yeast Set1, *Dictyostelium discoideum* Set1.

739 Ile2674 (in red) is highly conserved in all listed amino acid sequences.

740 Residues matching human KMT2B (grey), not matching (white), amino acids conserved in

741 all representative sequences (dark grey). ***** positions of fully conserved residues; **:**

742   conservation between groups of strongly similar properties and **.** conservation between

743   groups of weakly similar properties.

744   **Figure 2**
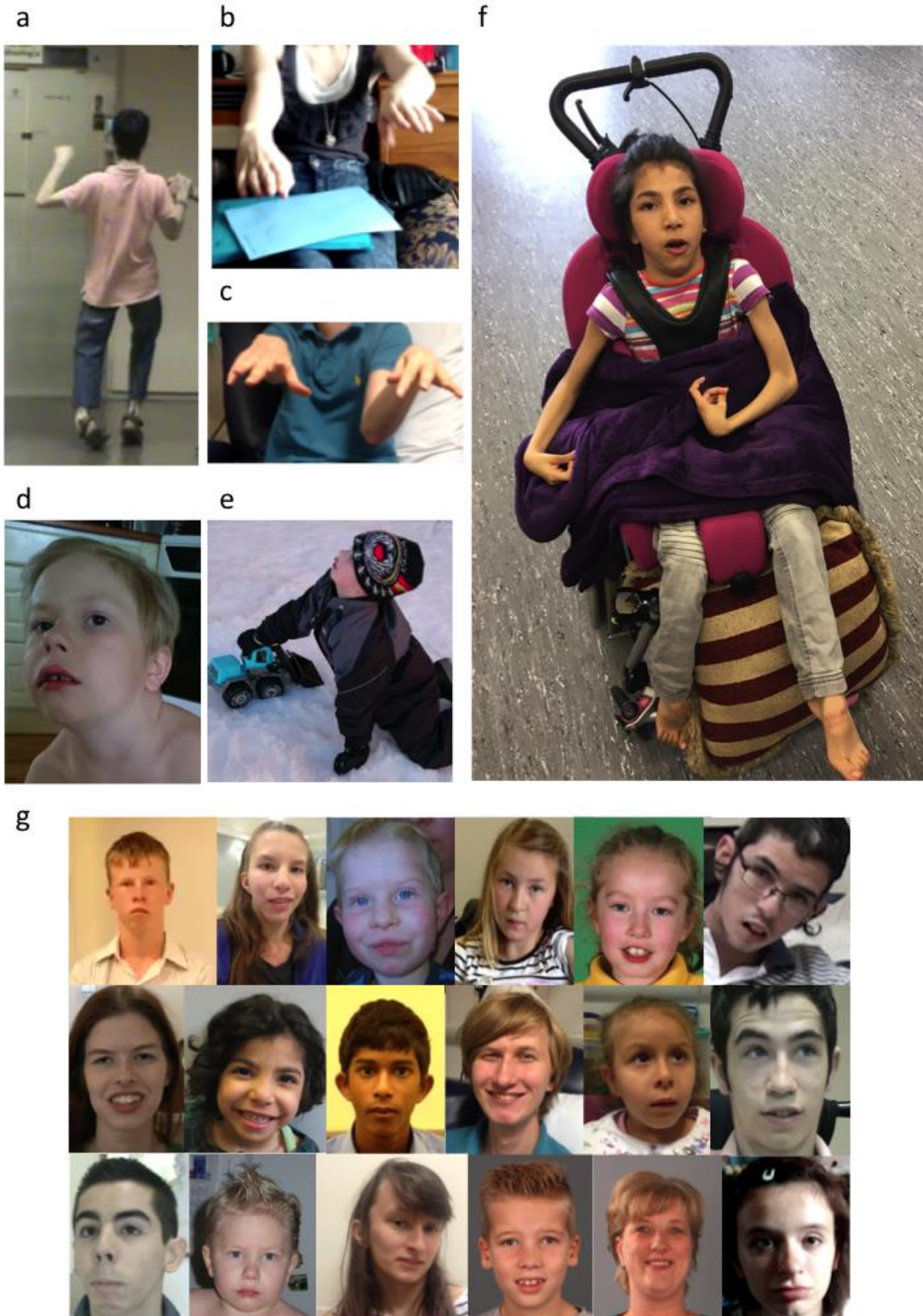
746

747 **Figure 2:**

748 **Clinical Features of Patients with *KMT2B* Mutations**

749 (**a**) Patient 17, age 13 years, evidence of gait disturbance with dystonic posturing of the

750 four limbs. (**b**) Patient 27, age 19 years and (**c**) Patient 14, age 18 years both showing

751 bilateral upper limb dystonic posturing. (**d, e**) Patient 23, age 8 years with retrocollis. (**f**)

752 Patient 12, age 6 years, generalized dystonia, with jaw-opening dystonia and 4-limb

753 posturing. (**g**) Montage of patient faces: Top row (left to right) Patients 1, 2, 3, 4, 8, 9;

754 Middle row (left to right) Patients 11, 12, 13, 14, 16, 17 and Bottom row (left to right)

755 Patients 21, 23, 25, 26a, 26b, 27. Facial elongation, broad nasal base and bulbous nasal

756 tip, particular evident in Patients 1, 2, 4, 9, 11, 12, 14, 17, 23, 25, 26a, 26b, 27.

757

758

759 **Figure 3**
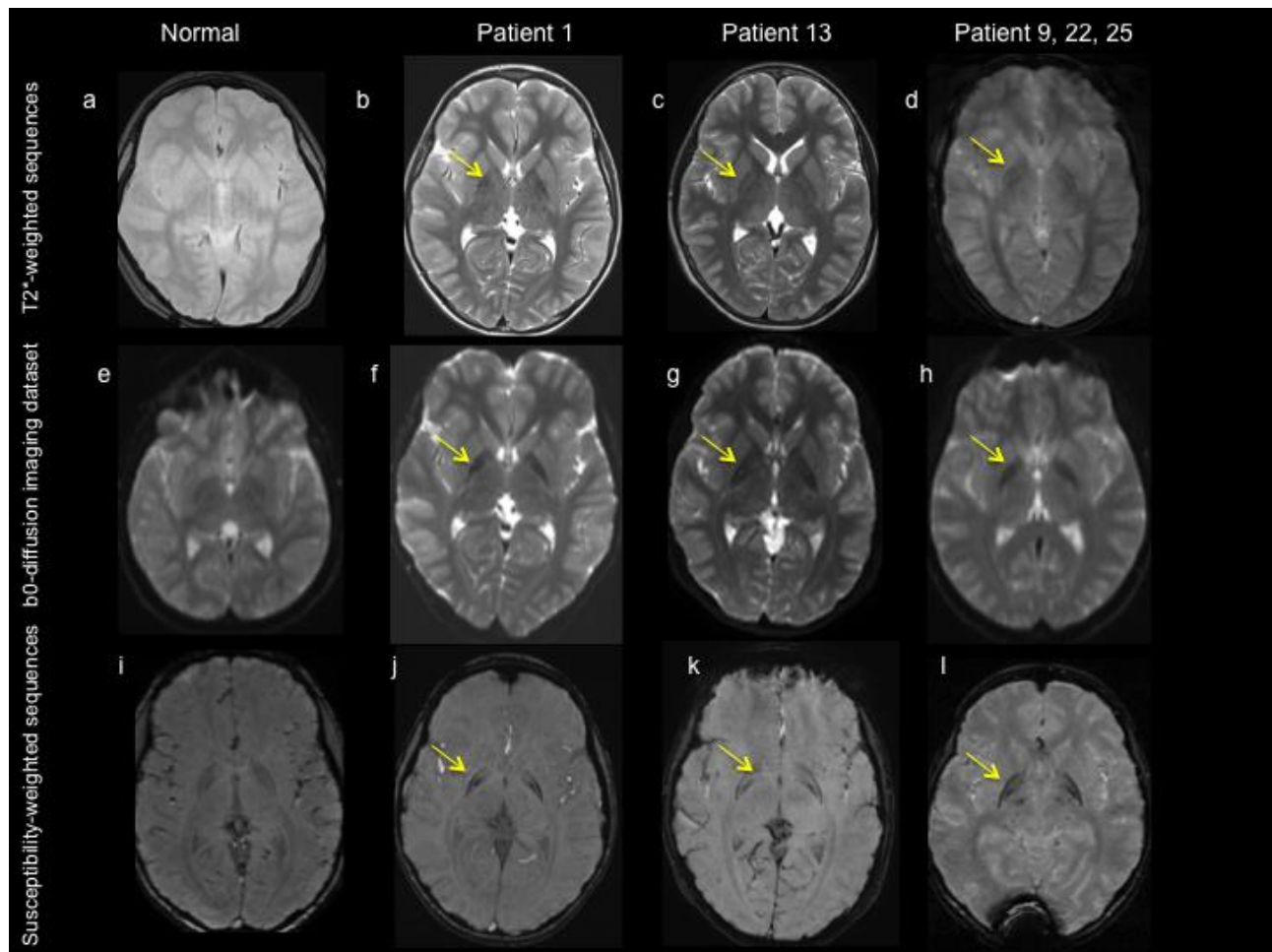
760

761 **Figure 3:**

762 **Radiological Features in KMT2B-patients**

763 Magnetic resonance imaging (MRI) with T2*-weighted sequences (**a-d**), diffusion- imaging

764 datasets with b-value of zero (**e-h**) and susceptibility weighted sequences (**i-l**). Abnormal

765 findings indicated by yellow arrows. (**a,e,i**) Representative MRI from control subjects for

766 T2*-weighted sequences (**a**: age 10y2m), diffusion-weighted sequences (**e**: age 10y4m)

767 and susceptibility weighted sequences (**i**: age 10y8m) indicating normal appearances of
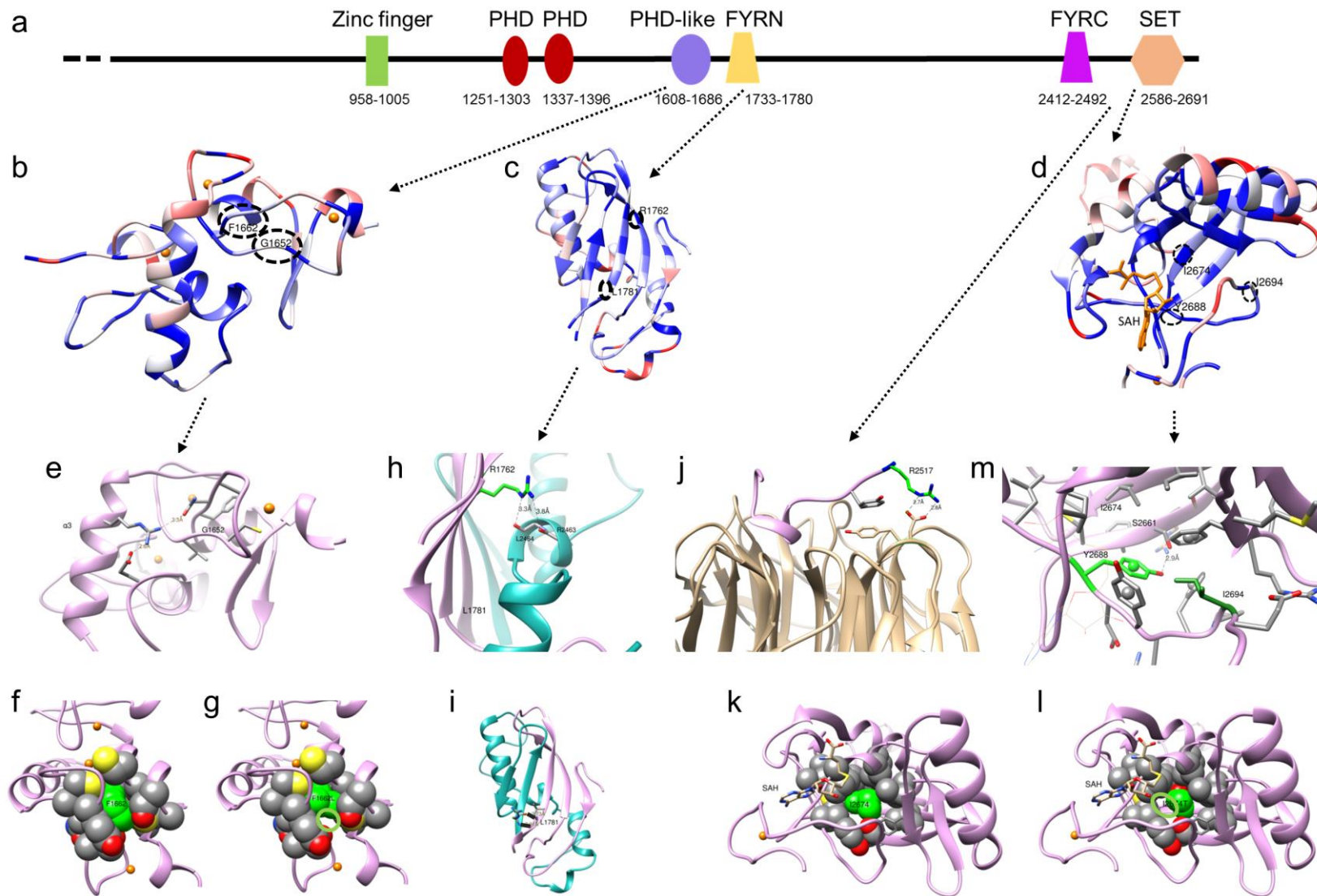
768 basal ganglia on all three sequences. (**b,f,j**) Patient 1, age 9y5m, (**c,g,k**) Patient 13, age

769 11y3m, (**d**) Patient 9, age 15y1m, (**h**) Patient 22 age 13y1m and (**l**) Patient 25, age 16y -

770   all show evidence of bilateral subtle hypointensity of the globus pallidus with hypointense

771   lateral streak of globus pallidus externa.

772 **Figure 4**

773

774 **Figure 4:**

775 **Homology Modelling of KMT2B Protein Structure**

776 (**a**) Schematic of domain architecture of KMT2B. (**b-d**) The degree of amino conservation

777 is displayed in the structural models for the different domains. Red to blue indicates

778 increasing conservation. (**b**) Model of PHD-like domain shows the mutation sites Gly1652

779 and Phe1662 (**c**) Model of the FYRN domain presents the position and conservation of

780 Arg1762 and Leu1781. (**d**) Model of the SET methyltransferase domain indicates the

781 position and conservation of Ile2674, Tyr2688 and Ile2694. (**e**) Location of Gly1652 in the

782 PHD-like domain model and the hydrogen bond network in the vicinity are shown. Helix α3

783 is also indicated. (**f**) Hydrophobic packing involving Phe1662 (green) is displayed. (**g**)

784 Change to leucine (green) at position 1662 is predicted to cause loss of contact within the

785 hydrophobic core. Residue side chains are presented as spheres highlighting van der

786 Waals contacts. (**h**) Interactions involving Arg1762 (green) from FYRN with Arg2463 and

787 Leu2464 of FYRC. The hydrogen bond interactions are highlighted. (**i**) Leu1781 shown at

788 the interface of FYRN (pink)/FYRC (blue) domains. The backbone hydrogen bonds

789 stabilizing the sheet structure are highlighted. (**j**) Interactions involving Arg2517 (green)

790 and WDR5 (brown). The salt bridge interaction between Arg2517 of KMT2B and Asp172

791 of WDR5 is highlighted. (**k**) Location and contacts involving Ile2674 (green) in the

792 hydrophobic core of the SET domain are exhibits. SAH is displayed in light brown. (**l**)

793 Conversion to threonine (green) at position 2674 is predicted to result in loss of contacts in

794 the core. (**m**) Interactions involving Tyr2688 (light green) and Ile2694 (dark green) in the

795 core of the SET domain. The hydrogen bond between Tyr2688 and Ser2661 is

796 highlighted.

797 **Figure 5**
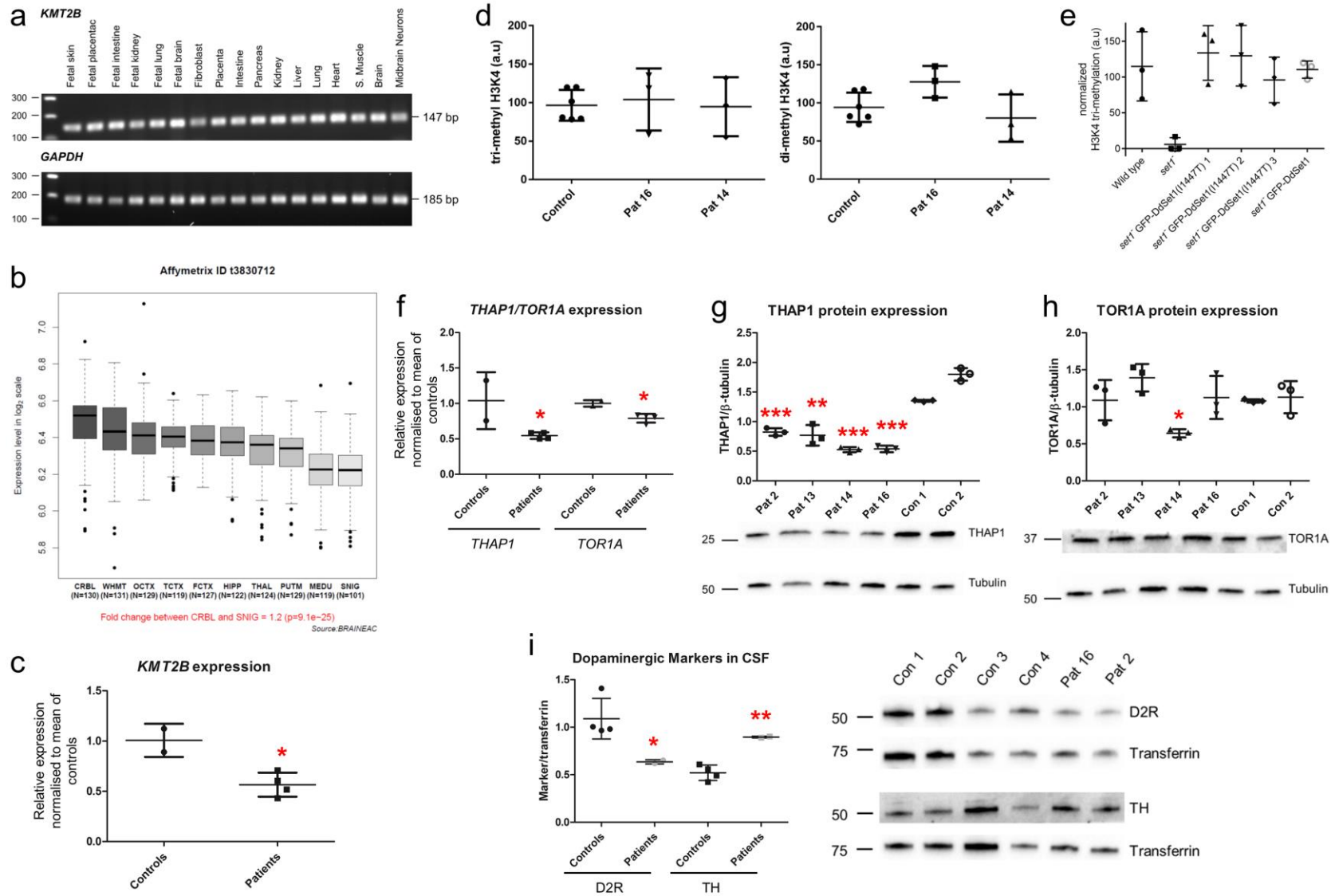
798

799 **Figure 5:**

800 **Functional Investigation of the Downstream Effects of Mutations in *KMT2B***

801 (**a**) PCR analysis of human fetal and adult cDNA for expression of *KMT2B. KMT2B* is

802 widely expressed in a range of human tissues, including fibroblasts, brain tissue and

803 midbrain dopaminergic neurons. (**b**) Box plots of *KMT2B* mRNA expression levels in 10

804 adult brain regions (source: BRAINEAC; http://www.braineac.org/). The expression levels

805 are based on exon array experiments as previously described and are plotted on a log2

806 scale (y axis)[49]. This plot shows that *KMT2B* is ubiquitously expressed across all 10 brain

807 regions analyzed, with expression higher in the cerebellum than in any other region.

808 Putamen (PUTM), frontal cortex (FCTX), temporal cortex (TCTX), occipital cortex (OCTX).

809 hippocampus (HIPP), substantia nigra (SNIG), medulla (specifically inferior olivary

810 nucleus, MEDU), intralobular white matter (WHMT), thalamus (THAL), and cerebellar

811 cortex (CRBL). "N" indicates the number of brain samples analyzed to generate the results

812 for each brain region. Whiskers extend from the box to 1.53 the interquartile range. (**c**)

813 Quantitative RT-PCR indicates that patients with *KMT2B* mutations (n=4) have

814 significantly decreased fibroblast mRNA levels of *KMT2B* when compared to controls

815 (Controls = 1.01±0.16SD, n=3 technical replicates of 2 biological samples; Patients =

816 0.57±0.12SD, n=3 technical replicates of 4 biological samples; two-tailed unpaired t-test,

817 p-value 0.0182). (**d**) Quantification of immunoblotting of tri-methyl H3K4 (left) and di-

818 methyl H3K4 (right) in histones extracted from patient-derived fibroblasts (Patient 14 and

819 16), and two control fibroblast cell lines. Methylation values are normalized to pan-histone

820 H3 levels. Individual data-points are plotted with center bar showing mean and error bars

821 showing standard deviation. Differences between control and patient-derived samples are

822 not significant (H3K4me3: Controls = 96.63±19.98SD; Patient 16 = 104.1±40.31SD;

823 Patient 14 = 94.75±38.36SD; p=0.62; H3K4me2: Controls = 94.33±19.25SD; Patient 16 =

824 127.8±20.79SD; Patient 14 = 80.23±31.09SD; p=0.07). n=3 fibroblast samples (technical

825 replicates). (**e**) Quantification of immunoblotting of tri-methyl H3K4 in *Dictyostelium* cell

826 lysates. Tri-methyl H3K4 intensity values are normalized against levels of total histone H3.

827 H3K4 tri-methylation is impaired in set1- cells compared to wild type. Expression of GFP-

828 DdSet1 or GFP-DdSet1(Ile1447Thr) in set1- cells rescues levels of H3K4Me3. Individual

829 data-points are plotted with center bar showing mean and error bars showing standard

830 deviation (Wild type = 115±48.25SD; set1- = 5.94±9.37SD; set1- GFP-DdSet1(I1447T) 1 =

831 133.7±38.11SD; set1- GFP-DdSet1(I1447T) 2 = 129.8±42.34SD; set1- GFP-

832 DdSet1(I1447T) 3 = 96.07±31.82SD; set1- GFP-DdSet1 = 110.5±12.02SD). n=3 samples

833 (technical replicates). (**f**) Quantitative RT-PCR of *THAP1* and *TOR1A*, indicates that

834 patients have a reduction of *THAP1,* and to a lesser extent of *TOR1A* transcripts in

835 comparison to controls (*THAP1:* Controls = 1.04±0.40SD, n=3 technical replicates of 2

836 biological samples; Patients = 0.55±0.05SD, n=3 technical replicates of 4 biological

837 samples; two-tailed unpaired t-test, p-value 0.0498; *TOR1A:* Controls = 1.00±0.05SD, n=3

838 technical replicates of 2 biological samples; Patients = 0.79±0.06SD, n=3 technical

839 replicates of 4 biological samples; two-tailed unpaired t-test, p-value 0.0140). (**g**)

840 Immunoblotting studies in fibroblasts indicate a significant reduction in THAP1 for Patient

841 2, 13, 14 and 16 when compared to controls (Control 1 = 1.34±0.02SD; Control 2 = 1.80±

842 0.11SD; Patient 2 = 0.83±0.06SD; Patient 13 = 0.77±0.17SD; Patient 14 = 0.53±0.04SD;

843 Patient 16 = 0.54±0.06SD; Kruskal-Wallis test, p-value 0.0078). n=3 fibroblast protein

844 samples (technical replicates). (**h**) Immunoblotting studies in fibroblasts indicate a

845 statistically reduced level of TOR1A in Patient 14 when compared to controls (Control 1 =

846 1.08±0.02SD; Control 2 = 1.13± 0.22SD; Patient 14 = 0.64±0.05SD; two-tailed unpaired t-

847 test, p-value 0.0196), but not for Patient 2, 13 and 16 (Patient 2 = 1.09±0.27SD; Patient 13

848 = 1.39±0.18SD; Patient 16 = 1.13±0.29SD; Kruskal-Wallis test, p-value 0.0812). n=3

849 fibroblast protein samples (technical replicates). (**i**) CSF immunoblotting studies on Patient

850   2 and 16 show markedly reduced levels of D2R and increased levels of TH when

851   compared to control CSF (D2R: Controls = 1.09±0.21SD, n=4 control CSF samples

852   (biological replicates); Patients = 0.64±0.02SD, n=2 patient CSF samples (biological

853   replicates); two-tailed unpaired t-test, p-value 0.0471; TH: Controls = 0.52±0.08SD, n=4

854   control CSF samples (biological replicates); Patients = 0.90±0.01SD, n=2 patient CSF

855   samples (biological replicates); two-tailed unpaired t-test, p-value 0.0036).

356 **Table 1a: *KMT2B* Mutations and Evolution of Motor Phenotype in KMT2B-dystonia**

Pat	Age (y) Sex M/F	*KMT2B* mutation[1]	Symptoms at presentation: Body distribution & motor features	Onset of dystonia (y)	Bilateral LL involve-ment (y)	Bilateral UL involve-ment (y)	Onset of cranial, cervical, laryngeal dystonia (y)	Symptoms of cranial, cervical, laryngeal dystonia	Trial of medication and clinical response	Deep brain stimulation (DBS)
1	14 M	Deletion: Chr19: 35,608,666-36,233,508	RLL Right foot posturing Gait disturbance	4	6	6-11	5	Dysarthria Dysphonia Swallowing difficulties	L-dopa trial – no benefit	No
2	14 F	Deletion: Chr19: 35,197,252-38,140,100	Bilateral LL Limping Gait disturbance	7	7	8-11	8	Dysarthria Dysphonia Drooling	L-dopa trial – no benefit BLF – no benefit	No
3	9 M	Deletion: Chr19: 34,697,740-37,084,510	RLL Right foot posturing Gait disturbance	2.5	3	6-7	4	Dysarthria Dysphonia Swallowing difficulties Drooling	GBP – some reduction in tone	No
4	11 F	Deletion: Chr19: 36,191,100-36,376,860	LLL Left toe walking Gait disturbance	4	8	9-12 m	5	Dysarthria Dysphonia Swallowing difficulties Drooling	L-dopa trial– minimal benefit THP – minimal benefit	Planned for 2016
5	20 M	Deletion: Chr19: 31,725,360-36,229,548	Developmental delay Gait disturbance	Present but age of onset not known	Present but age of onset not known	Present but age of onset not known	Not known	Nasal voice	None	No
6	10 F	Deletion: Chr19: 35,017,972-36,307,788	RLL Right foot inversion	2.5	4	4	4-7	Dysarthria/Anarthria Jaw-opening dystonia Swallowing difficulties NGF 6y PEG 8y Torticollis Severe retrocollis	L-dopa trial – no benefit THP – no benefit	Inserted age 7y Sustained excellent clinical benefits 3y post-DBS, marked improvement in torticollis, retrocollis, manual abilities and left leg dystonia. Loss of efficacy when 'DBS off' for almost a year and functional recovery when switched on again.
7	21 M	Deletion: Chr19: 35,414,997-37,579,142	RLL Right foot dragging Gait disturbance	7	7-8	13	13	Dysarthria Dysphonia Swallowing difficulties	L-dopa trial – no benefit BLF – no benefit	No

357

358

Pat	Age (y) Sex M/F	*KMT2B* mutation[1]	Symptoms at presentation: Body distribution & motor features	Onset of dystonia (y)	Bilateral LL involvement (y)	Bilateral UL involvement (y)	Onset of cranial, cervical, laryngeal dystonia (y)	Symptoms of cranial, cervical, laryngeal dystonia	Trial of medication and clinical response	Deep brain stimulation (DBS)
8	17 F	Deletion: Chr19: 35,414,997-37,579,142	RLL Right foot posturing	4	6	4-12	2.5	Dysarthria Dysphonia Drooling Torticollis	L-dopa trial – no benefit	Inserted age 10y Good response over 6 years, particularly evident after replacement of faulty right DBS lead
9	14 M	Deletion: Chr19: 35,967,904-37,928,373	Bilateral LL Gait disturbance	4	4	9-13	9	Dysarthria Dysphonia	L-dopa trial – possible initial benefit but not sustained	Inserted age 14y Very good clinical response at 4m post DBS with restoration of independent ambulation
10	7 F	Deletion: Chr19: 35,794,775-38,765,822	Bilateral LL Intermittent toe walking Gait disturbance	4	4	-	-	-	None	No
11	25 F	c.399_400insT p.Pro134Serfs*24	RUL Right Hand Cramps and Posturing	6	12	12	14[2]	Anarthria Orolingual dystonia Tongue thrusting Swallowing difficulties PEG	L-dopa trial – poorly tolerated, no benefit	Being considered
12	6 F	c.1690C>T p.Arg564*	Bilateral LL Toe walking	4	5	6	5	Dysarthria Swallowing difficulties	L-dopa trial – no benefit	No
13	11 M	c.3026_3027del p.Glu1009Glyfs*9	Bilateral UL Posturing, tremor Difficulty handwriting	8	9-10	8	9	Dysarthria Dysphonia	L-dopa trial – no benefit	No
14	18 M	c.3143_3149del p.Gly1048Glufs*132	Bilateral UL Posturing of hands Myoclonic jerks	8	13	8	13	Dysarthria Dysphonia Swallowing difficulties	L-dopa trial – no benefit	No
15	20 F	c.4545C>A p.Tyr1515*	Bilateral LL Toe Walking Clumsy	2	9	9	8.5	Dysarthria Dysphonia Oromandibular dystonia Swallowing difficulties PEG 18y	Moderate responses to (and currently taking) THP CLZ L-dopa BLF	No

359

Pat	Age (y) Sex M/F	*KMT2B* mutation[1]	Symptoms at presentation: Body distribution & motor features	Onset of dystonia (y)	Bilateral LL involve-ment (y)	Bilateral UL involve-ment (y)	Onset of cranial, cervical, laryngeal dystonia (y)	Symptoms of cranial, cervical, laryngeal dystonia	Trial of medication and clinical response	Deep brain stimulation (DBS)
16	6 F	c.4688del p.Ala1563Aspfs*83	Bilateral LL Increasing falls Gait disturbance	3	3	5	6	Dysarthria Dysphonia	L-dopa trial – no benefit THP – initial benefit, not sustained	No
17	17 M	c.6515_6518delins p.Val2172Alafs*11.	Bilateral LL Toe walking Gait disturbance	1	1	8	12	Dysarthria Dysphonia Swallowing difficulties	L-dopa trial – no benefit TBZ – no benefit BLF and THP – mild benefit	Inserted age 16y Very good clinical response 4m post-DBS with restoration of independent ambulation
18	20 F	c.8061del p.Tyr2688Thrfs*50	Clumsy movements Difficulties with speech articulation	1	-	-	Infancy	Dysarthria Dysphonia Swallowing and chewing difficulties	No	No
19	28 M	c.8076del p.Ile2694Serfs*44	Bilateral LL Toe walking Severe speech delay	2	3	4 (L>R)	7	Anarthria Jaw opening dystonia Tongue protrusion Swallowing difficulties PEG 8y L torticollis,R laterocollis	L-dopa trial – no benefit THP and TBZ reduced tongue protrusion	Inserted age 27y Improvement of jaw opening dystonia and tongue protrusion
20	40 M	c.3528+2T>A	LLL Gait disturbance L foot dragging Clumsiness	4	5	8	10	Severe dysarthria Dysphonia L Torticollis	L-dopa trial – no benefit TBZ, THP, SUL – no benefit	Inserted age 32y – no benefit. Electrode replaced in 2009 with sustained improvement in foot posture but only transient benefit to cervical, UL and LL dystonia.
21	18 M	c.4955G>A p.Gly1652Asp	RLL Right leg posturing	6	8	12	5	Dysarthria Dysphonia Swallowing difficulties	L-dopa trial – no benefit THP – not tolerated	Inserted age 15y Sustained clinical benefit 3y post-DBS, improved dystonia and independent walking
22	20 F	c.4986C>A p.Phe1662Leu	RLL Right foot posturing Abnormal gait	5	8	5-13	5-6	Dysarthria Dysphonia Swallowing difficulties Torticollis	L-dopa trial – no benefit BLF – no benefit THP – low dose, mild benefit BTX neck – reduction in pain but no functional	Inserted age 20y Very good clinical response 9m post DBS with improved dystonia and independent walking

361

							benefit			
Pat	**Age (y)** **Sex M/F**	***KMT2B* mutation[1]**	**Symptoms at presentation: Body distribution & motor features**	**Onset of dystonia (y)**	**Bilateral LL involve-ment (y)**	**Bilateral UL involve-ment (y)**	**Onset of cranial, cervical, laryngeal dystonia (y)**	**Symptoms of cranial, cervical, laryngeal dystonia**	**Trial of medication and clinical response**	**Deep brain stimulation (DBS)**
23	8 M	c.5114G>A p.Arg1705Gln	Bilateral LL Toe-walking	3	3	6	6.5	Dysarthria Torticollis	L-dopa trial – no benefit CLZ, THP, IT BLF – some benefit	Inserted age 7y with considerable benefit
24	27 F	c.5284C>T p.Arg1762Cys	LLL Tiptoe walking and in-turning of L foot	6	6	7	7	Dysarthria Anarthria from 14-15y Reduced tongue movements Swallowing preserved	L-dopa trial – no benefit THP- no benefit	No
25	19 F	c.5342T>C p.Leu1781Pro	RLL Right foot posturing Gait disturbance	8	12	13	10	Dysarthria Dysphonia Swallowing difficulties Torticollis	L-dopa trial – no benefit LVT – mild benefit	Inserted age 19y Very good clinical response 4m post-DBS with improved dystonia and ambulation[3]
26a	8 M	c.7549C>T p.Arg2517Trp	Delayed speech Delayed motor development	-	-	-	8	Severe paroxysmal retrocollis and jaw dystonia	-	No
26b	46 F	c.7549C>T p.Arg2517Trp	Bilateral UL UL posturing Torticollis Inability to walk long distances and run	23	26	23	23	Dysphonia Torticollis	None	No
27	19 F	c.8021T>C p.Ile2674Thr	RUL Posturing, tremor Difficulty handwriting Myoclonic jerks	9	11-13	10	9-10	Dysphonia	L-dopa trial – no benefit THP – no benefit LVT – no benefit CBZ – initial benefit, not sustained CLZ – not tolerated	No

362 BLF: baclofen; BTX: botulinum toxin; CLZ: clonazepam; GBP: gabapentin; IT: intrathecal; LL: lower limbs; LLL: left lower limb; LVT: levetiracetam; m: months; NGF: nasogastric feeding;
363 Pat: patient; PEG: percutaneous endoscopic gastrostomy; RLL: right lower limb; RUL: right upper limb; SUL: sulpiride; UL: upper limbs; TBZ: tetrabenzine; THP: trihexyphenidyl; y: years
364 [1] based on NCBI Reference Sequence: NM_014727.2
365 [2] onset shortly after being fitted with orthodontic braces
366 [3] had undergone 2 posterior cranial fossa explorations and palatal surgery before DBS

367 **Table 1b: Additional Clinical Features in KMT2B-patients**

Patient	*KMT2B* mutation	Number of genes in microdeletion	Intellectual disability	Dysmorphic features	Additional neurological features	Psychiatric features	Abnormal skin features	Other systemic manifestations
1	Deletion: Chr19: 35,608,666-36,233,508	38	Mild	Elongated face	Not reported	Not reported	Not reported	Not reported
2	Deletion: Chr19: 35,197,252- 38,140,100	124	No	Elongated face Bulbous nasal tip	Not reported	Not reported	Not reported	Not reported
3	Deletion: Chr19: 34,697,740 -37,084,510	109	Moderate	Elongated face	Not reported	Not reported	Cutis aplasia[1]	Retinal dystrophy
4	Deletion: Chr19: 36,191,100-36,376,860	14	V mild - subtle memory problems	Elongated face Broad nasal bridge Bulbous nasal tip	Not reported	Prone to anxiety[2]	Not reported	Not reported
5	Deletion: Chr19: 31,725,360-36,229,548	110	Moderate	Sparse hair Blepharophimosis Absent eyelashes of lower eyelids Low set, posteriorly rotated ears Epicanthic folds Narrow nasal bridge, ridge and point Largely bifid tongue Micrognathia Teeth overcrowding Finger contractures 5th finger clinodactyly Toe over-riding Dysplastic toenails	Microcephaly	Not reported	Occipital cutis aplasia	Small echogenic kidneys with low GFR, required renal transplant at 17 years
6	Deletion: Chr19: 35,017,97-36,307,788	69	No	Not reported	Microcephaly	Not reported	Not reported	Not reported
7	Deletion: Chr19: 35,414,997-37,579,142	99	Mild	Elongated face	Absence seizures	Not reported	Not reported	Absent right testis
8	Deletion: Chr19: 35,414,997-37,579,142	99	Mild	5th finger clinodacytly	Not reported	Not reported	Ectodermal dysplasia	Not reported
9	Deletion: Chr19: 35,967,904-37,928,373	79	Mild	Elongated face	Strabismus	Not reported	Not reported	Cleft palate
10	Deletion: Chr19: 35,794,775-38,765,822	111	Moderate	Not reported	Strabismus	Not reported	Not reported	Short stature Bronchiectasis

368

Patient	*KMT2B* mutation	Number of genes in microdeletion	Intellectual disability	Dysmorphic features	Additional neurological features	Psychiatric features	Abnormal skin features	Other systemic manifestations
11	c.399_400insT p.Pro134Serfs*24	-	No	Bulbous nasal tip	Not reported	Not reported	Not reported	Not reported
12	c.1690C>T p.Arg564*	-	Moderate	Elongated face Bulbous nasal tip, short nasal root, Hypertelorism, large mouth with full lower lip	Epilepsy	Not reported	Not reported	Not reported
13	c.3026_3027del p.Glu1009Glyfs*9	-	V mild - difficulties with attention	Elongated face	Not reported	Not reported	Not reported	Not reported
14	c.3143_3149del p.Gly1048Glufs*132	-	No	Elongated face Bulbous nasal tip	Not reported	Not reported	Not reported	Not reported
15	c.4545C>A p.Tyr1515*	-	No	Elongated face Bulbous nasal tip	Not reported	Not reported	Not reported	Not reported
16	c.4688del p.Ala1563Aspfs*83	-	No	Elongated face	Not reported	Not reported	Not reported	Not reported
17	c.6515_6518delins p.Val2172Alafs*11.	-	No	Elongated face	Not reported	Not reported	Phimosos	Short stature
18	c.8061del p.Tyr2688Thrfs*50	-	Mild	Micrognathia Atrophic tongue Bulbous nasal tip 5th finger clinodacytly	Not reported	Not reported	Not reported	Not reported
19	c.8076del p.Ile2694Serfs*44	-	No	Short stature	Delay in saccade initiation and hypometric vertical saccades	ADHD[3] with no response to Ritalin	Not reported	Not reported
20	c.3528+2T>A	-	Moderate 6y- verbal IQ 74 Performance IQ 87 No cognitive decline	Not reported	Not reported	Not reported	Not reported	Not reported
21	c.4955G>A p.Gly1652Asp	-	Mild	Elongated face	Not reported	Not reported	Not reported	Short stature Hypertrichosis
22	c.4986C>A p.Phe1662Leu	-	No	Elongated face Bulbous nasal tip	Not reported	Not reported	Not reported	Not reported

370
371

Patient	*KMT2B* mutation	Number of genes in microdeletion	Intellectual disability	Dysmorphic features	Additional neurological features	Psychiatric features	Abnormal skin features	Other systemic manifestations
23	c.5114G>A p.Arg1705Gln	-	Mild-moderate 6y WISC-IV 50-60	Elongated face Bulbous nasal tip Broad philtrum, Upslanted eyes, epicanthus, low-set ears, periorbital fullness, gap between front teeth	Spasticity in lower limbs from 6y	Not reported	Ichtyotic skin lesions with criss-cross pattern under the feet and at knees, broad scarring after operation	Episodic vomiting
24	c.5284C>T p.Arg1762Cys	-	No	Short stature	Oculomotor apraxia with difficulty initiating saccades. Mild spasticity	No	Not reported	Not reported
25	c.5342T>C p.Leu1781Pro	-	No	Elongated face Bulbous nasal tip	Not reported	Not reported	Not reported	Not reported
26a	c.7549C>T p.Arg2517Trp	-	No	Bulbous nasal tip	None	ADHD[3] Currently on methyphenidate, oxazepam, risperidone	Not reported	Not reported
26b	c.7549C>T p.Arg2517Trp	-	No	Bulbous nasal tip	Idiopathic intracranial hypertension – on acetazolamide	None	Not reported	Not reported
27	c.8021T>C p.Ile2674Thr	-	V subtle mild learning difficulties	Bulbous nasal tip	Not reported	Anxiety Self-harm behavior Depression Obsessive-compulsive traits[4]	Not reported	Not reported

372
373 [1] Supplementary Figure 3c
374 [2] Identified on formal psychology review
375 [3] Diagnosed by psychiatrist and under regular psychiatry review
376 [4] Under regular review with psychiatrist (ICD-10-CM F06.30; ICD-10-CM F42)
377 ADHD: attention deficit hyperactivity disorder; GFR: glomerular filtration rate; V: very; y: years